The XPS of Pyridine: A Combined Theoretical and Experimental Analysis

Paul S. Bagus[a]*, Connie J. Nelin[b], Michel Sassi[c], Daniel Baranowski[c], Marcus A. Sharp[c], Tom Autrey[c], Zdenek Dohnálek[c,d], and Zbynek Novotny[c]

[a]Department of Chemistry, University of North Texas, Denton, TX 76203-5017, USA

[b]Consultant, Austin, TX 78730, USA

[c]Physical and Computational Sciences Directorate, Pacific Northwest National Laboratory, Richland, WA 99352, USA

[d]Voiland School of Chemical Engineering and Bioengineering, Washington State University; Pullman, Washington 99163, USA.

*Author to whom correspondence should be addressed: Paul.Bagus@unt.edu

Abstract:

A detailed analysis of the N(1s) and C(1s) X-Ray Photoelectron Spectroscopy, XPS, is made where the measured XPS is compared with theoretical Sudden Approximation, SA, intensities and theoretical XPS Binding Energies, BEs. There is remarkably good agreement between the theoretical predictions and the measured XPS; in particular, the different Full Width at Half Maximum, FWHM, for the C(1s) and N(1s) BEs is explained in terms of unresolved C(1s) BEs for the different C atoms in pyridine. This work demonstrates that the combination of theory and XPS measurements can extract analysis of the XPS relevant to the molecular electronic structure. The theory used is based on fully relativistic self-consistent field solutions of the Dirac-Coulomb Hamiltonian and the SA is used to determine relative XPS intensities.

Keywords: XPS Spectra, Binding Energies (BEs), △SCF Theory, Sudden Approximation (SA)

I. Introduction:

X-Ray Photoelectron Spectroscopy, XPS, has a long history as a powerful method to identify not only elemental composition but also the electronic structure of the material studied. This can already be seen in the pioneering work of the Uppsala group directed initially by Siegbahn. [1, 2] Theory, especially rigorous *ab initio* theory, is an important complement for the interpretation of measured XPS and is regularly used; an early effort to demonstrate the application of theory to the core hole states generated in XPS is the paper by Bagus. [3] While it is not possible to cite the vast number of papers that apply theory for the interpretation of XPS, two recent reviews by the present authors [4, 5] do cite much of this literature. In this paper, the goal of extracting chemical information from XPS measurements is addressed with a combined experimental and theoretical analysis of the XPS of a simple organic molecule, pyridine, with the formula C_5NH_5. Our interest in pyridine and CNH materials in general arises from our investigations of the chemical transformation of molecules adsorbed on N-doped graphene surfaces. [6] N-doped carbon materials are reported to activate molecular hydrogen to transfer to and from heterocyclic arene of liquid organic hydrogen carriers, LOHCs, such as pyridine and quinoline. [7-9] LOHCs are a unique class of 'hydrogen energy carriers' that show promise to store and transport large quantities of green hydrogen for large-scale and long-duration energy storage applications. [10, 11] We are using a combination of computational and spectroscopic approaches to gain insight into the fundamental interactions of molecules at N-doped graphene surfaces. The objective is to determine how the properties of the surfaces and the adsorbates can be modified in order to optimize the desired reactivity. XPS provides the ability to characterize both the surface of N-doped carbon materials and molecules adsorbed to the surface.

In pyridine, the main features of the XPS spectrum are a single N(1s) XPS peak and three C(1s) XPS peaks for the three inequivalent C atoms in the molecule. A high resolution C(1s) XPS spectrum of pyridine, obtained using synchrotron radiation and with a photon energy of 382 eV, [12] clearly show that each non-symmetrically equivalent C can be resolved. While the authors of Mendolicchio *et al.* [12] used a photon energy of 382 eV to obtain this high-resolution C(1s) spectra, it came with two essential limitations. First, they were not able to access the N(1s) ionization, where the BE is 400.18 eV. Second, for the C(1s) ionization, which can be probed with 382 eV photons, the photoelectron has a kinetic energy of less than 100 eV. This low energy photo-electron represents an issue as the usual XPS analyses, which are based on the sudden approximation, [13] cannot be performed because these analyses are exact only in the limit of infinite photon energy. However, the sudden approximation is still valid for photon energies of Al K_α X-Rays [14] as used in the present paper. As the focus of this paper is to compare the broadening and underlying chemistry for both the C(1s) and N(1s) peaks, it is important to have an experiment which can measure both and which can be accurately described using the sudden approximation. While Mendolicchio *et al.* [12] argue that it is necessary to include vibronic effects to describe the details of their high-resolution C(1s) spectra obtained with low energy photons, there is strong evidence [1, 2, 13, 15, 16] that this is not important at the usual high energy Mg or Al K_α. Indeed, the vibrational effects lead only to a minor broadening of the XPS features. [15] Here, our concern is about the different broadening of the C(1s) and N(1s) XPS peaks, as reflected in the Full Width at Half Maximum (FWHM), which is accurately described by our measurements and by our theoretical analysis. A particular advantage of our theoretical analysis is that we are able to identify the intensities and energies of XPS BEs that cannot be obtained with the resolution of the measurements.

In our study, the XPS measurements are made on a thin film of pyridine and the theory is based on *ab initio* fully relativistic self-consistent field wavefunctions, WFs, for the initial, ground state (GS), and the core ion states that involve removal of a localized 1s electron from the N and C atoms. The principal objective is to show that this combination results in a detailed analysis and interpretation of the XPS. The analysis includes reliable estimates of the experimental resolution and of the BE shifts which, for the C(1s) XPS feature, lead to a broadening of this XPS peak. This broadening is accurately given from the theoretical BE shifts and theoretical XPS intensities of the individual C(1s) ionizations. It is demonstrated that a general methodology and protocol is described that should have wide applicability.

In the following section, Section II Geometry, Measurements and Methodology, we describe the pyridine molecular geometry and the experimental and theoretical methodologies. This is followed in Section III, XPS BEs and Intensities, with a presentation of our XPS measurements coupled with the theoretical results for BEs and intensities. In particular, the excellent agreement of measurement and theory is stressed. Finally, in Section IV, our conclusions are summarized.

II. Geometry, Measurements and Methodology:

A schematic of the pyridine molecule is given in Figure 1 where the different atoms are identified and labeled as: N, C1, C2L, C2R, C3L and C3R. The two equivalent C3 carbon atoms are the carbon atoms closest to N with C3L and C3R being on the left-hand side and the right-hand side, respectively; see Figure 1. The two equivalent C2L and C2R atoms are next nearest the N atom and the C1 atom is furthest from N. The H atoms, H1, H2L, H2R, H3L, and H3R, are labeled according to the C atom they are associated with. The molecule is planar and placed in the xy plane. The coordinates used for the atoms were obtained from the NIST database. [17] The coordinates used are given in Table 1.

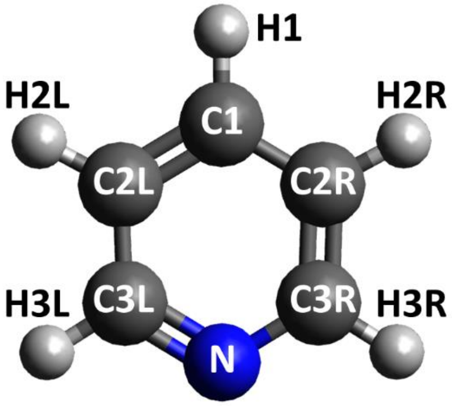

Figure 1: The geometry of the pyridine molecule, C_5NH_5, where the different atoms are labelled so that they can be referenced in the text. The labelling distinguishes symmetrically equivalent and inequivalent C and H atoms.

	X	**Y**	**Z**
N	+0.0	+1.43026	0.0
C1	+0.0	-1.392063	0.0
C2	±1.1995239	-0.673874	0.0
C3	±1.1481118	+0.725329	0.0
H1	+0.0	-2.487089	0.0
H2	±2.1619982	-1.192724	0.0
H3	±2.0753331	+1.309391	0.0

Table 1: Coordinates of the atoms in the pyridine molecule, in Å; the x coordinate for equivalent C atoms is shown with a ± sign. For the labeling of the atoms see Figure 1.

The wavefunction, WF, calculations were carried out in C_s symmetry where only the reflection in the xy plane was taken into account. This is done to allow the 1s ionizations of the equivalent pairs of C2 and C3 atoms to be localized on either the left or right of the equivalent atoms. For localization of the core ions of equivalent atoms see, for example, Refs [18, 19]. The WFs, and orbitals were calculated as self-consistent Dirac Hartree-Fock solutions with the Dirac-Coulomb Hamiltonian. The orbitals are complex four-component solutions for the C_s^* double group and with all terms including Large-Large, LL, Large-Small, LS, Small-Small, SS, and Gaunt included; see Saue *et al*. [20] The ground, initial, state has 21 doubly occupied spin-orbitals and there are no exact degeneracies although there are near degeneracies, especially for the C2 and C3 1s levels. The WFs for six 1s ions are also calculated. Here the configurations have a singly occupied 1s orbital on one of the N or C atoms and 20 doubly occupied orbitals. The orbitals and WFs are optimized for these six configurations. The pairs for C(1s) ions of the localized C2L and C2R have identical total energies as well as the pair with the localized C3L and C3R C(1s) ions. However, the two sets of orbitals and WFs for these pairs were calculated to confirm that they were indeed identical. For an ideal localized 1s orbital, the expectation value of $\mathbf{r}$, $\langle\mathbf{r}\rangle$, would be equal to the coordinates of the C atom that it is localized about. To confirm the degree of localization, the $\langle\mathbf{r}\rangle$ was calculated for the singly occupied orbital localized about the C3L carbon atom and found to be $\langle\mathbf{r}\rangle=(-1.148,+0.725,0.0)$ which is indeed the position of the C3L atom, see Table 1.

The theoretical 1s ionization potential or BE is the difference of the total energies of the ground state, GS, and the localized 1s ion:

$$\mathrm{BE(1s, atom) = E(1s\ ion, atom) - E(GS)}, \qquad (1)$$

where the sign is chosen so that BE>0. These BEs are described as ΔSCF BEs and it is known that they are accurate BE values compared to XPS measurements; see, for example, Refs. [4, 5]. However, it is necessary to be aware of one limitation in terms of comparing calculated BEs to measured BEs which have been obtained for condensed materials or thin films. While the reference energy for the theory has the vacuum energy as zero, the reference for the measurements may be different, either a Fermi level or a reference for a known material; see, for example Brundle *et al.* [21]. The ΔSCF BE includes what are described as relaxation energies, E_R, which take into account the response of the orbitals, especially the valence shell orbitals, to the fact that a core hole is present. The frozen orbital BE is found by simply annihilating a core orbital from the GS WF; for a closed shell GS, this is the negative of the Hartree-Fock orbital energy of the closed shell and is denoted BE(KT) = $-\varepsilon$. [22] The E_R is simply the difference of the BE(△SCF) and BE(KT):

$$E_R = \mathrm{BE}(\Delta\mathrm{SCF}) - \mathrm{BE}(\mathrm{KT}). \quad (2)$$

The XPS relative intensities, I_{rel}, are obtained with the sudden approximation, SA, developed by Aberg, [13, 16] and generally used for the calculation of XPS intensities from theoretical WFs; see, for example, Ref. [4]. The sudden approximation is based on the overlap of the WFs for the states of the core ion, Ψ(ion), with the initial state where the core orbital has been annihilated, denoted as $a_i^\dagger\Psi(\mathrm{GS})$, and where suitable sums are taken over different degenerate or near-degenerate states. [4] The situation is particularly simple for pyridine where there is a non-degenerate initial GS and very limited degeneracy in the ionic states. Here, the SA are normalized such that the sum of I_{rel} for the ionization of one of the core levels over its main and all satellite peaks is 1. However, our concern is only for the I_{rel} of the main peak which will be less than 1. For the comparison with the experiment, it is necessary to broaden the directly computed BEs to the ionic states in order to take into account experimental resolution and lifetime broadening. This is done with a Voigt convolution [23] of a Gaussian which represents experimental resolution and a Lorentzian which represents broadening due to the lifetime of the core ion. The specific values used in the Voigt convolutions are discussed and justified when the results are presented in the following section. Calculations of the orbitals and WFs were performed with a slightly modified version of the relativistic DIRAC program system. [20, 24] The calculations of the XPS intensities were made with programs in the CLIPS program package [25] where the output of DIRAC has been interfaced to CLIPS. Programs were written for the Voigt broadening of the XPS. The basis set exponents are given in the Supporting Information (SI).

The XPS measurements were performed using a standard Omicron EA125 electron analyzer equipped with 7 channeltron detectors and non-monochromatized Al Kα X-rays produced by Omicron DAR400 source. The base pressure in the XPS system was $2.0\text{x}10^{-10}$ Torr. For the XPS measurements, no charge compensation was used. Pyridine (Alfa Aesar, 99.5%) has been purified by freeze-pump-thaw cycles and dosed as a thick multilayer film (equivalent to 50 monolayers) using a molecular beam onto a sample held at 100 K. The multilayer film was deposited on a half-metallic iron oxide, $Fe_3O_4(001)$, single crystal. XPS spectra were collected at normal emission using a pass energy of PE=10 eV to ensure higher resolution. This resolution was estimated by using the same experimental parameters (50 meV step size, 1 s dwell time, same anode, analyzer slits and pass energy), and measuring the FWHM of Au 4f 7/2 peak to be 1.11 ± 0.01 eV. The stoichiometry of our pyridine films was confirmed to be that expected for molecular pyridine by the following method. We varied the coverage and observed the same stoichiometry for a monolayer film dosed with a molecular beam where the C:N stoichiometry was found to be 4.99 ± 0.02. This monolayer film was measured before depositing more molecules on top to obtain multilayer coverage. Further, since we observe the same stoichiometry for both monolayer and multilayer coverage, we can conclude that the role of adventitious carbon is negligible.

III. XPS BEs and Intensities:

In Table 2, the theoretical and measured XPS BEs for the N(1s) and C(1s) ions are presented. For each of the distinct atoms, the atom and the number of equivalent atoms is given following the notation in Figure 1. For each atom, the BE(△SCF) and the E(R) are given in eV; the BE shifts from the lowest C atom, △BE(△SCF), are also given. From the XPS measurements, the C(1s) and N(1s) BE(XPS) and the △BE(XPS) are given. There is only one resolved C(1s) XPS BE; the different broadening of the XPS N(1s) and C(1s) peaks will be discussed later.

	# equivalent	**BE(△SCF)**	**△BE(△SCF)**	**E(R)**	**BE(XPS)**	**△BE(XPS)**
C2(1s)	2	290.68	0.00	15.5		
C1(1s)	1	291.21	0.53	15.4	286.27	0.00
C3(1s)	2	291.59	0.91	15.5		
N(1s)	1	404.48	113.80	19.4	400.18	113.91

Table 2: For the inequivalent atoms, see Figure 1, theoretical C(1s) and N(1s) BE(△SCF), relaxation energies, E(R) and BE shifts, △BE(△SCF) are given; the reference energy for the △BE(△SCF) is the lowest C(1s) BE for the C2 atoms. The number of symmetrically equivalent atoms is also given. For the XPS, the BE(XPS) and △BE(XPS) are given. All energies are in eV.

The C(1s) BEs span a small energy range of less than 1 eV and they will not be resolved, especially with our non-monochromatic XPS. They will, however, lead to a broadening of the C(1s) peak as we will show shortly. The relaxation energies are very similar, within 0.1 eV, and this is to be expected given the very similar environments for all the C atoms. The N(1s) BE(△SCF) is 113 to 114 eV larger than the C(1s) BE, entirely as expected given the larger nuclear charge for N. It is, however, important that the N(1s) △BE(△SCF) and the measured △BE(XPS) are remarkably similar. This is the case even though the absolute values of the BE(XPS) are about 5 eV smaller than the BE(△SCF) which is simply because a different reference than vacuum zero is used for the BE(XPS). This indicates that our theoretical treatment of the 1s BEs is satisfactory and that the SA I_{rel} which are needed to compare to the experimental XPS are reliable. The SA I_{rel} and the intensity lost from the main peak, which is observed, to satellites, which are not observed, are given in Table 3.

	$\mathbf{I_{rel}}$	**% Loss**
C2(1s)	1.381	30.9
C1(1s)	0.690	31.0
C3(1s)	1.357	32.2
N(1s)	0.669	33.1

Table 3: SA I_{rel} to the C(1s) and N(1s) main XPS peaks; the loss to satellites is also shown as a percentage which is simply $100x(1-I_{rel})$. The I_{rel} for C2 and C3 are greater than 1 because they are for ionization of two equivalent atoms.

The N(1s) and C(1s) I_{rel} will be broadened, rigidly shifted, scaled, and compared to the experiment. From the data in Table 3, the departures from the intensity ratio for C2:C1:C3 of 2:1:2 based on the number of equivalent atoms of each type is rather small. This is simply because the losses of intensity from the main peaks to satellites are very similar for all three types of C atoms;

see Table 3. The loss from the main N(1s) peak to satellites is similar to that of the C atoms; this is true since the nuclear charges of C and N differ by only 1 and they have similar chemical bonding.

Now, we turn now to plots of the Voigt broadened theory with the XPS experiment. The comparison for the N(1s) is shown in Figure 2 where the XPS is shown as a dashed blue curve and the broadened theory is shown as a solid black curve. The N(1s) XPS is taken with a pass energy E_P=10 eV and a Shirley background [26] is subtracted. The Voigt broadening parameters are a Lorentzian with Full width at Half Maximum, FWHM of 0.093 eV for the lifetime taken from the compendium of Campbell and Papp [27] and a Gaussian with a 1.2 eV FWHM for experimental resolution. The Gaussian was chosen to give a good fit between the theoretical and measured N(1s) XPS curves. However, it is a reasonable estimate for experimental resolution. This Gaussian FWHM was also used to broaden the C(1s) BEs. The theory and measured XPS were scaled so that they both had a scaled intensity of 0.98 at their maxima and they were rigidly shifted so that their maxima were at E_{rel}=0.0 eV. There is reasonable agreement between theory and XPS measurement, but this is not surprising since there is only one N(1s) BE which needs to have a dominantly Gaussian broadening for since the lifetime broadening is rather small and increases the overall FWHM by only 0.06 eV; see Figure 2. The main value of the comparison of theory and measurement for the N(1s) is that it provides a reasonable value to use for the Gaussian broadening for the C(1s) XPS. However, we note there is a modest asymmetry of the fit of the Gaussian (solid curve) and the XPS measurement (dashed curve). For E_{rel}~1 eV, the Gaussian curve is slightly too broad compared to the measured XPS and for somewhat greater E_{rel}~1.5-2 eV, the Gaussian is too narrow. This is because we have used a single Gaussian to fit the spectrum which contains contributions from the nearly degenerate $K\alpha_1$ and $K\alpha_2$ X-Rays which are split by 0.4 eV.

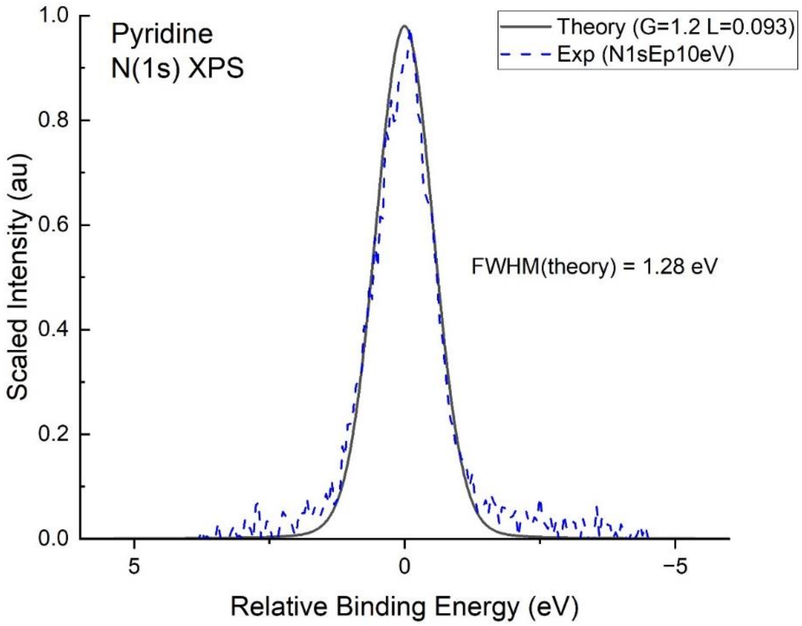

Figure 2: Plot comparing measured N(1s) XPS, dotted curve, and the Voigt broadened theoretical BE, full curve; Gaussian (G) and Lorentzian (L) FWHM for the Voigt broadening are shown and the experimental EP is indicated. See text for an explanation of the scaling and shifts applied to align theory and experiment.

The theory and XPS for the unresolved C(1s) XPS are shown in Figure 3 where many of the conventions and parameters are the same as for the N(1s) comparison in Figure 2. A major difference is that there are three underlying broadened C(1s) peaks with energy shifts and intensities as given in Tables 2 and 3, respectively. These curves are shown in color and the full theoretical black curve is the sum of the three curves for the different C(1s) ionizations. The Voigt broadening of the individual C(1s) curves uses the same Gaussian FWHM of 1.2 eV as used for the N(1s) curve and the Lorentzian broadening for the C(1s) lifetime has a FWHM of 0.06 eV. [27] The measurement for the C(1s) is taken with an EP=10 eV to ensure even better resolution and the background removal is also made with a Shirley approach. The key point is that the three unresolved C(1s) contributions lead to an overall theoretical FWHM of 1.72 eV which is almost in exact agreement with the XPS measurement, which is represented by a dashed curve in Figure 3.

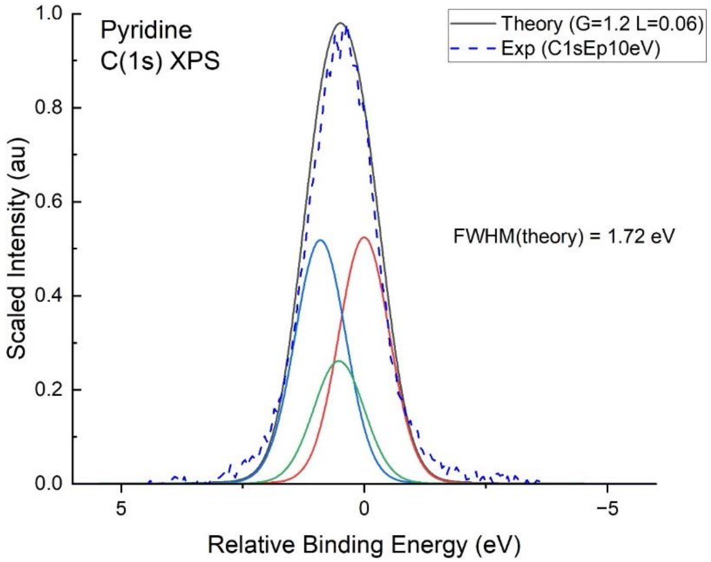

Figure 3: Plot comparing measured C(1s) XPS, dotted curve, and the Voigt broadened theoretical BE, full curve. The individual C(1s) contributions are shown as colored curves beneath their sum, the full curve. Parameters are as described as for Figure 2.

IV. Conclusions:

We have presented a detailed, combined theoretical and experimental, analysis of the N(1s) and C(1s) XPS of pyridine. While the N(1s) is a single peak, the C(1s) is a modestly broader peak arising from the contributions of three unresolved peaks from the three inequivalent C atoms in pyridine. Without the theoretical input for the C(1s) BE shifts and intensities, it would not be possible to make a deconvolution of the measured C(1s) XPS peak into the three individual contributions. On the other hand, without the measured N(1s) XPS, it would be difficult to make a reasonable estimate of the appropriate FWHM for the Gaussian broadening to represent the experimental resolution. We recall that while FWHM of the Lorentzian lifetime broadening are well known [27] the FWHM of the Gaussian broadenings depend strongly on the parameters of the XPS measurement. They need to be either determined through separate measurements or to be extracted from an analysis of the XPS spectrum; in the present work we have used the latter for our analysis of the spectra. This insight is a step towards our goal of characterizing the environment in proximity to the pyridinic nitrogen functional groups in two-dimensional carbon materials doped with nitrogen. In particular, our work has shown how XPS can be used to provide information that allows us to reach this goal. It is especially impressive that the theory and measured XPS are in excellent agreement. The absolute measured and theoretical BEs disagree by about 5 eV with theoretical BEs being larger; this is because the reference values for theory and measurement are not the same. However, for the difference of the C(1s) and N(1s) BEs, i.e., the BE shift, the theory and measurement are in excellent agreement. This is a very strong measure of the reliability of the △SCF theoretical method to provide reliable BE shifts for the analysis of the measured XPS, especially for molecular systems similar to pyridine. In particular, while there are likely to be small errors in the theoretical absolute values of the BEs since the SCF energies do not take account of electron correlation effects in the core, 1s, shell; [28] this error will be essentially the same for the N(1s) and C(1s) BEs. Overall, an important conclusion of this work is that it demonstrates the reliability of our theoretical analysis based on a △SCF approach and which includes fully the relativistic effects.

Supplementary Material

This material contains the exponents for the Gaussian basis functions used for the Pyridine wavefunction calculations. Since the basis set is fully uncontracted, there is no contraction information.

Acknowledgements

PSB gratefully acknowledges support from the U.S. Department of Energy, Office of Science, Office of Basic Energy Sciences, Chemical Sciences, Geosciences, and Biosciences (CSGB) Division through its Geosciences program, FWP 56674 at Pacific Northwest National Laboratory (PNNL). TA, MS, DB, ZD, and ZN acknowledge support from the U.S. Department of Energy, Office of Science, Basic Energy Sciences, Physical Behavior of Materials under Award No. 80110. DB and MAS acknowledge support from the U.S. Department of Energy, Office of Science, Basic Energy Sciences, Chemical Sciences, Geosciences, and Biosciences Division, Catalysis Science Program, FWP 47319. PNNL is a multi-program national laboratory operated for the DOE by Battelle Memorial Institute under contract no. DE-AC05-76RL01830.

Conflict of Interest

The authors have no conflicts of interest.

Author Contributions

Paul S. Bagus: Data curation; Formal analysis; Methodology; Writing – original draft; Writing – review & editing.

Connie J. Nelin: Data curation; Formal analysis; Methodology; Writing – review & editing.
Michel Sassi: Conceptualization; Writing – review & editing.

Daniel Baranowski: Data curation; Formal analysis; Writing – review & editing.

Marcus A. Sharp: Data curation; Formal analysis; Writing – review & editing. **Tom Autrey:** Funding acquisition; Resources; Writing – review & editing.

Zdenek Dohnálek: Data curation; Writing – review & editing.

Zbynek Novotny: Data curation; Formal analysis; Writing – review & editing.

Data Availability Statement

The data that supports the findings of this study are available within the article and its supplementary information.

References:

[1] K. Siegbahn, C. Nordling, G. Johansson, J. Hedman, P.F. Hedén, K. Hamrin, U. Gelius, T. Bergmark, L.O. Werme, R. Manne, Y. Baer, ESCA-Applied to Free Molecules North-Holland, Amsterdam 1969.
[2] K. Siegbahn, C. Nordling, A. Fahlman, R. Nordberg, K. Hamrin, J. Hedman, G. Johansson, T. Bergmark, S.E. Karlsson, I. Lindgren, B. Lindberg, ESCA-Atomic, Molecular, and Solid State Structure Studied by Means of Electron Spectroscopy, Almqvist and Wiksells, Uppsala, Sweden, 1967.
[3] P.S. Bagus, Self-Consistent-Field Wave Functions for Hole States of Some Ne-Like and Ar-Like Ions, Phys. Rev. 139 (1965) A619-A634.
[4] P.S. Bagus, C.J. Nelin, C.R. Brundle, Chemical significance of x-ray photoelectron spectroscopy binding energy shifts: A Perspective, J. Vac. Sci. Technol., A 41 (2023) 068501.
[5] P.S. Bagus, E.S. Ilton, C.J. Nelin, Extracting Chemical Information From XPS Spectra: A Perspective, Catal. Lett. 148 (2018) 1785-1802.
[6] P.S. Rice, G. Lee, B. Schwartz, T. Autrey, B. Ginovska, Leveraging Curvature on N-Doped Carbon Materials for Hydrogen Storage, Small 20 (2024) 2310162.
[7] H. Hu, Y. Nie, Y. Tao, W. Huang, L. Qi, R. Nie, Metal-free carbocatalyst for room temperature acceptorless dehydrogenation of N-heterocycles, Science Advances 8 (2022) eabl9478.
[8] Z. Luo, R. Nie, V.T. Nguyen, A. Biswas, R.K. Behera, X. Wu, T. Kobayashi, A. Sadow, B. Wang, W. Huang, L. Qi, Transition metal-like carbocatalyst, Nat. Commun. 11 (2020) 4091.
[9] W.J. Shaw, M.K. Kidder, S.R. Bare, M. Delferro, J.R. Morris, F.M. Toma, S.D. Senanayake, T. Autrey, E.J. Biddinger, S. Boettcher, M.E. Bowden, P.F. Britt, R.C. Brown, R.M. Bullock, J.G. Chen, C. Daniel, P.K. Dorhout, R.A. Efroymson, K.J. Gaffney, L. Gagliardi, A.S. Harper, D.J. Heldebrant, O.R. Luca, M. Lyubovsky, J.L. Male, D.J. Miller, T. Prozorov, R. Rallo, R. Rana, R.M. Rioux, A.D. Sadow, J.A. Schaidle, L.A. Schulte, W.A. Tarpeh, D.G. Vlachos, B.D. Vogt, R.S. Weber, J.Y. Yang, E. Arenholz, B.A. Helms, W. Huang, J.L. Jordahl, C. Karakaya, K. Kian, J. Kothandaraman, J. Lercher, P. Liu, D. Malhotra, K.T. Mueller, C.P. O'Brien, R.M. Palomino, L. Qi, J.A. Rodriguez, R. Rousseau, J.C. Russell, M.L. Sarazen, D.S. Sholl, E.A. Smith, M.B. Stevens, Y. Surendranath, C.J. Tassone, B. Tran, W. Tumas, K.S. Walton, A US perspective on closing the carbon cycle to defossilize difficult-to-electrify segments of our economy, Nature Reviews Chemistry 8 (2024) 376-400.

[10] H. Breunig, F. Rosner, S. Saqline, D. Papadias, E. Grant, K. Brooks, T. Autrey, R. Ahluwalia, J. King, S. Hammond, Achieving gigawatt-scale green hydrogen production and seasonal storage at industrial locations across the U.S, Nat. Commun. 15 (2024) 9049.
[11] T. Autrey, P. Chen, Hydrogen energy carriers, Journal of Energy Chemistry 77 (2023) 119-121.
[12] M. Mendolicchio, A. Baiardi, G. Fronzoni, M. Stener, C. Grazioli, M. de Simone, V. Barone, Theory meets experiment for unravelling the C1s X-ray photoelectron spectra of pyridine, 2-fluoropyridine, and 2,6-difluoropyridine, J. Chem. Phys. 151 (2019).
[13] T. Aberg, Theory of X-Ray Satellites, Phys. Rev. 156 (1967) 35.
[14] B.D. Hermsmeier, C.S. Fadley, B. Sinkovic, M.O. Krause, J. Jimenez-Mier, P. Gerard, T.A. Carlson, S.T. Manson, S.K. Bhattacharya, Energy dependence of the outer core-level multiplet structures in atomic Mn and Mn-containing compounds, Phys. Rev. B 48 (1993) 12425-12437.
[15] P.S. Bagus, C.J. Nelin, Computation of Vibrational Excitations in XPS Spectroscopy, in: D.A. Penchoff, C.B. Sims, T.L. Windus (Eds.), Rare Earth Elements and Actinides: Progress in Computational Science Applications, American Chemical Society2021, pp. 181.
[16] R. Manne, T. Åberg, Koopmans' Theorm for Inner-Shell Ionization, Chem. Phys. Lett. 7 (1970) 282.
[17] NIST Chemistry Webook, SDR 69, (2023) DOI: https://doi.org/10.18434/T4D303.
[18] P.S. Bagus, H.F. Schaefer, III, Localized and delocalized 1s hole states of the O2+ molecular ion, J. Chem. Phys. 56 (1972) 224-226.
[19] P.S. Bagus, M. Schrenk, D.W. Davis, D.A. Shirley, Anomalous multiplet-splitting intensity ratios in K-level X-ray photoemission, Phys. Rev. A 9 (1974) 1090-1096.
[20] T. Saue, R. Bast, A.S.P. Gomes, H.J.A. Jensen, L. Visscher, I.A. Aucar, R.D. Remigio, K.G. Dyall, E. Eliav, E. Fasshauer, T. Fleig, L. Halbert, E.D. Hedegård, B. Helmich-Paris, M. Iliaš, C.R. Jacob, S. Knecht, J.K. Laerdahl, M.L. Vidal, M.K. Nayak, M. Olejniczak, J.M.H. Olsen, M. Pernpointner, B. Senjean, A. Shee, A. Sunaga, J.N.P.v. Stralen, The DIRAC code for relativistic molecular calculations, J. Chem. Phys. 152 (2020) 204104.
[21] C.R. Brundle, B.V. Crist, P.S. Bagus, Accuracy limitations for composition analysis by XPS using relative peak intensities: LiF as an example, J. Vac. Sci. Technol., A 39 (2021) 013202.
[22] R.S. Mulliken, J. chim. Phys. 46 (1949) 497.
[23] J.A. Gubner, A new series for approximating Voigt functions, J. Phys. A 27 (1994) L745-749.
[24] Dirac, a relativistic ab initio electronic structure program, Release DIRAC14 (2014), written by T. Saue, L. Visscher, H. J. Aa. Jensen, and R. Bast, with contributions from V. Bakken, K. G. Dyall, S. Dubillard, U. Ekström, E. Eliav, T. Enevoldsen, E. Faßhauer, T. Fleig, O. Fossgaard, A. S. P. Gomes, T. Helgaker, J. Henriksson, M. Iliaš, Ch. R. Jacob, S. Knecht, S. Komorovský, O. Kullie, C. V. Larsen, J. K. Lærdahl, Y. S. Lee, H. S. Nataraj, P. Norman, G. Olejniczak, J. Olsen, Y. C. Park, J. K. Pedersen, M. Pernpointner, R. di Remigio, K. Ruud, P. Sałek, B. Schimmelpfennig, J. Sikkema, A. J. Thorvaldsen, J. Thyssen, J. van Stralen, S. Villaume, O. Visser, T. Winther, and S. Yamamoto (see http://www.diracprogram.org).
[25] CLIPS is a program system to compute ab initio SCF and correlated wavefunctions for polyatomic systems. It has been developed based on the publicly available programs in the ALCHEMY package from the IBM San Jose Research Laboratory by P. S. Bagus, B. Liu, A. D. McLean, and M. Yoshimine.
[26] D.A. Shirley, High-resolution X-ray photoemission spectrum of the valence bands of gold, Phys. Rev. B 5 (1972) 4709-4714.
[27] J.L. Campbell, T. Papp, WIDTHS OF THE ATOMIC K - N7 LEVELS, Atomic Data and Nuclear Data Tables 77 (2001) 1-56.
[28] C.C.J. Roothaan, A.W. Weiss, Correlated Orbitals for the Ground State of Heliumlike Systems, Rev. Mod. Phys. 32 (1960) 194-205.